Pressure induced structural changes and dimer destabilization of HIV-1 protease studied by molecular-dynamics simulations.

Eva Kutálková, Josef Hrnčiřík and Marek Ingr*

Tomas Bata University in Zlín, Faculty of Technology, Department of Physics and Materials Engineering, Nám. T.G. Masaryka 5555, 76001 Zlín, Czech Republic

*Corresponding author: phone: +420 576031417, fax: +420 576035141, e-mail: ingr@ft.utb.cz

ABSTRACT

High-pressure methods became an attractive tool of investigation of structural stability of proteins. Besides protein unfolding, dimerization can be studied this way, too. HIV-1 protease is a convenient target of experimental and theoretical high-pressure studies. In this study molecular-dynamics simulations are used to predict the response of HIV-1 protease to the pressure of 0.1 to 600 MPa. The protease conformation of both monomer and dimer is highly rigid changing insignificantly with growing pressure. Hydrophobicity of the protease decreases with increasing pressure. Water density inside the active-site cavity grows from 87% to 100% of the bulk water density within the pressure range. Dimer-dissociation volume change is negative values for most of the pressure range with the minimum of –105 ml/mol, except a short interval of positive values at low pressures. The dimer is thus slightly stabilized up to 160 MPa, but strongly destabilized by higher pressures.

Keywords: HIV-1 protease, high pressure, molecular dynamics, dimerization equilibrium, volume change

1. INTRODUCTION

The protease of type-1 human immunodeficiency virus (HIV-1 PR) is one of the most studied enzymes in general. As an inevitable part of the life cycle of HIV virus, the causative agent of AIDS disease, this protein is an important therapeutic target in AIDS treatment. Therefore, a huge number of experimental studies in the fields of molecular biology, biochemistry and biophysics have been performed since the AIDS pandemics burst out which contributed to revealing the structure and enzymological properties of the enzyme. As a result of this effort, nine inhibitors have been brought to the stage of commercially produced and therapeutically used drugs during this period[1,2].

In addition to the experimental research, theoretical studies based on the methods of molecular dynamics and quantum chemistry have been carried out which also helped us to understand better the structure-function relationship within the enzyme and provided a valuable contribution to the drug development by means of rational drug design[3].

Structural stability is one of the thoroughly studied features of HIV-1 PR. The first study of this phenomenon was performed by Todd et al.[4] by differential scanning calorimetry, who presumed a tight connection between the dimer dissociation and unfolding. However, recent NMR experiments showed that the monomers of retroviral proteases of M-PMV[5], HIV-1 PR[6] and HIV-2 PR[7] can keep their structures even without the dimerization partners. The hypothesis of a stable HIV-1 PR monomer was supported also by the molecular-dynamics simulations by Levy et al.[8] and Yan et al.[9]. Unfolding of HIV-1 PR monomer facilitated by denaturing agents was studied by Noel et al.[10] who showed that certain mutations in the protease sequence increase its tendency to unfold. Molecular-dynamics simulations were carried out in order to explain the mechanism of monomer folding and characterize its intermediates[11,12].

As the enzyme is active as a homodimer, it was believed that an efficient inhibitor can be designed that disrupts the dimer formation and several experimental and theoretical studies were carried out with this aim[13]. Number of research teams made an effort to measure the dimerization equilibrium constant $K_d = [M]^2/[D]$, where $[M]$ is the concentration of monomer and $[D]$ of dimer[14-18]. Unfortunately, the results of these measurements differ by several orders of magnitude among the different studies in dependence on the used method, therefore the overall experimental evidence is so far inconclusive. An obvious cause of the experimental troubles is the high stability of the dimer and the subsequent necessity to do the experiments in very low concentrations in which the experimental sensitivity is limited by the low signal to noise ratio.

High-pressure methods represent a suitable way of studying thermodynamic transitions of biomolecules that cannot be easily observed at atmospheric pressure. Although the high-pressure conditions are non-physiological, they are often used in combination with several spectroscopic and other techniques in order to study the structural stability of proteins with respect to unfolding. Besides this, these techniques are an attractive tool to study equilibrium behavior of the oligomeric proteins or the active site structure and the mechanism of enzyme catalysis can be studied this way as well[19,20]. The necessary condition of applicability of the high-pressure methods is a negative volume change ΔV of the studied process in the direction that should be enforced by pressure increase.

Molecular dynamics simulations of proteins under high pressure have been carried out for various proteins, especially in order to study protein unfolding[21-26]. For the theoretical background overview see the review by Paci[27] discussing various aspects of high-pressure molecular-dynamics simulations including the usability of the standard force fields parameterized at atmospheric pressure. A reliable assessment of this problem is difficult since not many parallel experiments and calculations have been carried out and the accuracy of the experimental data is also limited[27]. In

general, all the intermolecular interactions are supposed to be well parametrized, especially in the attractive regions of the potential curves, in order to reproduce the atmospheric-pressure properties of the molecules correctly. Application of high pressure causes small changes of the mean intermolecular distances (at 600 MPa the linear intermolecular distances decrease approx. by 5%) and only insignificant internal-energy increase (pressure increase by 600 MPa increases the energy similarly as temperature increase by 10 K), therefore the molecules are not shifted out of the reliable potential range. Recently Lerbret et al.[28] compared the vibrational density of states of lysozyme and bulk water obtained both experimentally (inelastic neutron scattering) and theoretically (molecular dynamics) which resulted in a remarkably good agreement for both the systems. Calculations of ΔV have been reported for the process of unfolding of several proteins[21,24]. They are in general based on calculation of the difference of partial molar volumes (PMV) of the unfolded and folded system. A troublesome point of these calculations is that the volume change is often about 2 orders of magnitude lower than the volume fluctuations of the simulated system which results in errors of ΔV comparable to the value itself even when long sets of data are used. To our knowledge, this approach has not been used for evaluation of ΔV of pure dimer or oligomer dissociation yet.

Considering the HIV-1 PR dimerization, application of high pressure can help to enforce dimer dissociation which may facilitate the determination of K_d and enable further experiments with free monomers. However, to our knowledge no experimental and only one theoretical study[29] describing the behavior of HIV-1 PR under the conditions of high pressure have been published to date. In their work Meher et al. compare the HIV-1 PR dimer at atmospheric pressure and 300 MPa as regards the geometrical properties of the molecule.

In this study we use molecular dynamics simulations to get deeper insight in the high pressure response of HIV-1 PR in both dimeric and monomeric states. Simulations are carried out in the

pressure range from atmospheric pressure up to 600 MPa. The changes in geometry of the molecules are evaluated as well as the variability in interactions of the protein molecules with water. A special interest is dedicated to the water density in the active-site cavity which is also used as a base for the estimate of the volume change ΔV of the dimer dissociation as a function of pressure.

2. RESULTS AND DISCUSSION

2.1. Conformational changes of dimer and monomer of HIV-1 PR

Unrestrained, all-atom molecular dynamics simulations with the smaller water box initiated from both the closed and open conformations of protease dimer at atmospheric pressure suggested that closed, semi-open and open conformations are in dynamical equilibrium. The average life time of the individual conformation is in the order of nanoseconds. Semi-open form prevails in the statistical ensemble which agrees with the previously published data of Hornak et al.[30]. The same situation was observed also for the high pressure end of the studied interval, i.e. pressures of 500 and 600 MPa.

Simulations with the bigger water box were carried out for all the pressures under study (0.1, 100, 200, 300, 400, 500, 600 MPa) for the purpose of the comparative study of the different physical properties of the HIV-1 PR dimer. In order to select sufficiently equilibrated states of the protein at different pressures, conformational changes of the dimer and the backbone root mean square deviation (rmsd) were analyzed. Closed conformation states were chosen as starting points of the comparative study of all the investigated parameters as they keep the best conformational similarity over the whole pressure range. In addition, their ability of water repulsion is stronger in comparison with the semi-open and open conformations, which makes them more suitable for the calculations regarding hydrophobicity.

Figure 1 shows a typical closed conformation of the protein dimer and Figure 2 the evolution of a typical backbone rmsd of the dimer. As in the case of the smaller water box, the individual conformations are stable for several nanoseconds and are separated by relatively sharp transitions.

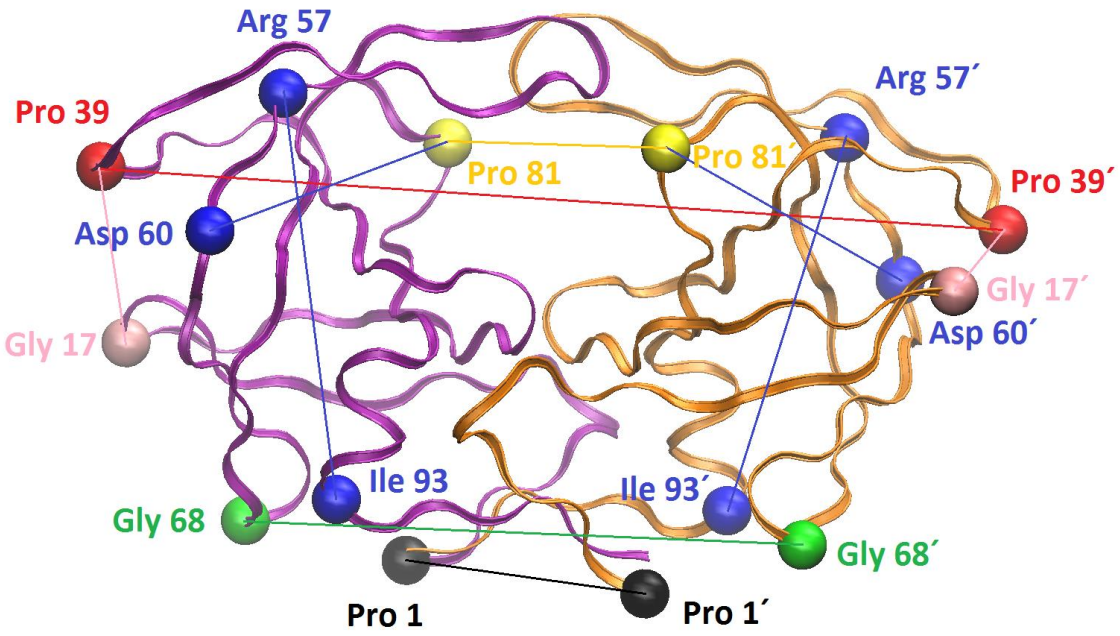

Figure 1. Distances of α-carbons of selected amino acids in the molecule of HIV-1 protease dimer.

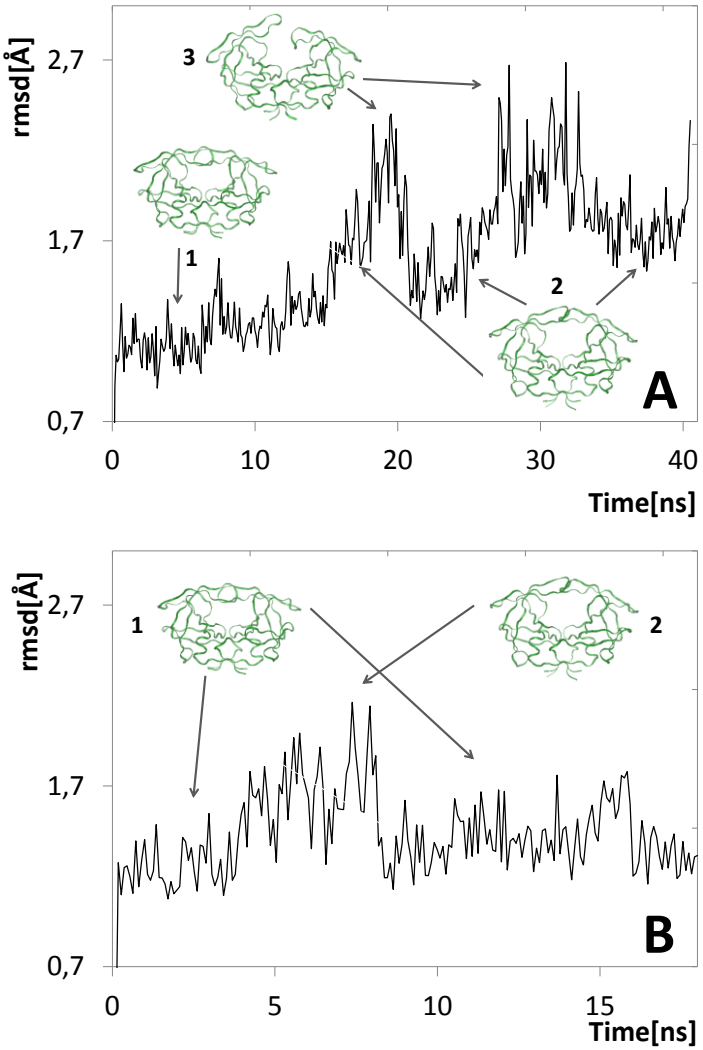

Figure 2. Root mean square deviation (rmsd) of a typical dimer simulation at atmospheric pressure. The stable regions of individual conformations as well as the transitions between them can be seen. A. Equilibrium of all three conformations, closed (1), semi-open (2) and open (3), during a 40-ns run. B. Equilibrium between closed (1) and semi-open (2) conformations in a different simulation. After the return of the system to the closed conformation (in approx. 8 ns), Na^+ ion was bound by Asp25 and 25' (in approx. 12 ns) which stabilizes the closed conformation.

Pressure induced structural changes of the HIV-1 protease dimer were investigated by the equilibrium MD simulations in the interval of 0.1 to 600 MPa. Evaluation of the characteristic

quantities were performed on well equilibrated parts of the simulation runs of 4.5 ns for dimer (closed conformation) and 9 ns for monomer. Figures S1, S2 show the rmsd profile of these parts of the simulations. It can be seen that the dimer structure keeps the rmsd values generally below 1.5 which indicates a considerably rigid structure. On the contrary, monomer structure seems to be somewhat looser with higher rmsd fluctuations but without significant rmsd drift. Volume, pressure and temperature fluctuations during the course of the simulation are shown in the Figure S3. The volume and pressure fluctuations are considerably lower than the differences of these quantities calculated for an arbitrary pair of the selected pressures. The amplitude of the volume fluctuations decreases with growing pressure, while the fluctuations of pressure and temperature are pressure independent.

In accord with the previous study[29] a tiny shrinkage of the structure can be observed at high pressure, but no dramatic change can be seen within the typical simulation time. The general change of the structure can be characterized by the pressure dependence of the radius of gyration (Figure 3). It decreases slowly and monotonously

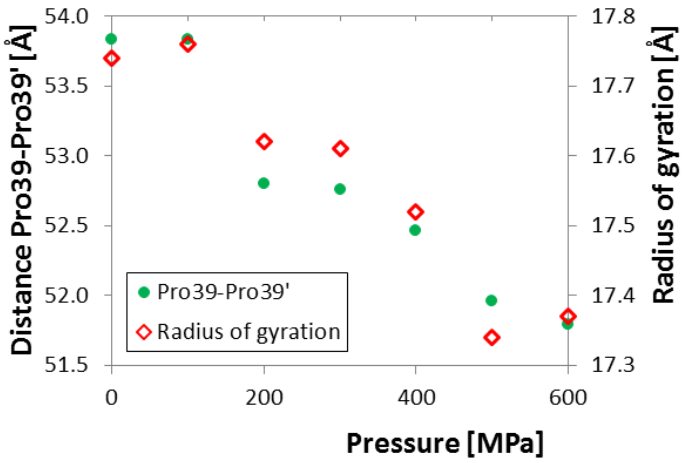

Figure 3. Distance of Pro39–Pro39' α-carbons and radius of gyration of the dimer. Standard deviations of the mean of the individual points do not exceed 0.1% of the absolute values as a consequence of averaging over large data sets. Minor inhomogeneities in the trends are caused by small differences of the protein conformations in different simulations.

across the whole pressure range by approx. 2.0%. In order to find out which parts of the molecule are mostly responsible for this change, several linear dimensions between topologically significant atoms of the molecule were measured. The distances are shown in Figure 1 and their values are listed in Table 1. It can be seen that the distance of the α-carbons of prolines 39 and 39′ (the non-primed and primed numbers are used to distinguish between the two monomers) situated at the outermost points of the structure in a turn familiarly called "ear" by Perryman et al. 2004[31], decreases in a remarkable accordance with the radius of gyration (Figure 3). The distance shrinks from original 53.8 Å at atmospheric pressure to 51.8 Å at 600 MPa, i.e. by approx. 3.7%. Distance shortening is observed also for the "ear" and "cheek", i.e. Gly 17 and Pro 39 of the same subunit, but the data are rather scattered and the trend is not so clear. In contrast with this, other distances between significant points of the structure do not show any remarkable change (Table 1). This is,

Table 1. Distances of α-carbons of selected amino acids in the molecule of HIV-1 protease dimer and monomer.

pressure [MPa]	distance [Å]								
	dimer							monomer	
	Pro39–Pro39' ("ears")	Pro81–Pro81' (cavity)	Gly68–Gly68'	Gly17–Pro39 ("cheek" – "ear")	Pro1–Pro1' ("whiskers")	Asp60 – Pro81	Arg57 – Ile93	Asp60 – Pro81	Arg57 – Ile93
0.1	53.83	21.15	35.55	12.37	17.51	21.8	23.9	21.8	23.8
100	53.83	21.50	36.63	11.95	16.47	21.7	23.7	21.6	23.4
200	52.80	21.05	34.62	11.77	17.38	21.7	23.5	21.8	23.3
300	52.76	20.87	34.88	11.97	17.80	21.7	23.5	21.7	23.0
400	52.46	20.51	34.33	11.41	17.57	21.7	23.4	21.7	23.5
500	51.96	19.37	34.88	11.66	16.91	21.6	23.0	21.3	23.3
600	51.79	22.15	34.79	11.58	17.38	21.5	23.1	21.5	23.7

for instance, the case of the distance between Gly 68 and 68′ situated at the turn close to the

dimerization domain, and the distance between Pro 1 and 1′ in the dimerization domain at the "whiskers". Both do not show any noticeable trend and only randomly oscillate around their mean values. Even the distance between prolines 81 and 81' located directly at the inner surface of the active-site cavity does not express a monotonous trend, but rather big oscillations during the time course of the simulation. Hence, the molecule seems to be a relatively rigid structure changing its conformation only in the less firmly fixed parts of the surface. The overall structure of the molecule resists even very high pressures without significant changes. This is particularly true for the dimerization domain composed of the intertwined ends of both monomer subunits. Even the active-site cavity is not much sensitive to the pressure, but its dimensions change with the conformation oscillations that occur during the time at any selected pressure.

Two characteristic distances were determined also for monomer (blue lines in Figure 1). One of them, the distance between the α-carbons of Arg57 and Ile93, runs from the flap to the dimerization domain, while the other one, Asp60 to Pro81 α-carbons distance, is approximately perpendicular to it. These two distances (Table 1) are almost pressure independent with only tiny fluctuations around their mean values. Moreover, there is no change between these distances in the dimer and monomer structures. At 600 MPa a partial distortion of the geometry can be observed which may indicate an initiation of the pressure induced unfolding of monomers. The monomer molecule thus seems to be a well-defined structure keeping its conformation irrespective of the dimerization state. This observation, therefore, is in agreement with the NMR study of Ishima et al.[6] that confirmed the existence of stable free HIV-1 PR monomers, and even extends this conclusion to the high-pressure conditions. However, at some simulation runs small structural distortions in the monomer structure were observed for 600 MPa indicating the possible initiation of the pressure induced unfolding of the monomers.

Water-accessible surface area of the monomer and dimer molecules was calculated as an auxiliary

geometrical indicator. The result is shown in Figure 4. For dimer the decrease of this area is

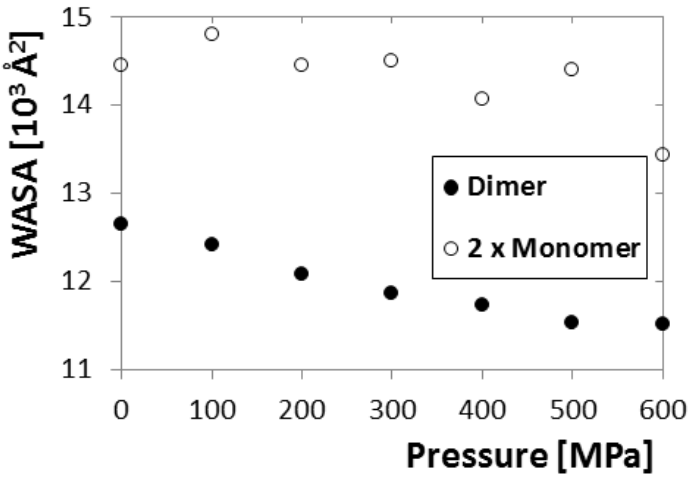

Figure 4. Water accessible surface area (WASA) of monomer and dimer. The value for monomer is multiplied by 2. Standard deviations of the mean of the individual points do not exceed 0.1%.

monotonous within the whole pressure range, while for monomer the decrease is much lower and biased by fluctuations. At 600 MPa it decreases more significantly, probably as a consequence of the partial structural collapse described previously as a possible initiation of a pressure-induced unfolding of a monomer. The size of water-accessible surface area reflects the slight shrinkage of dimer molecule indicated by radius of gyration and the Pro39-Pro39´ distance, but decreases only insignificantly for monomer. This is in accord with the other geometrical parameters and confirms the low adaptability of both the structures to high pressure.

2.2. Interaction of HIV-1 PR with water and water density in the active-site cavity

Interaction of the protein molecule with water may play the principal role in the dimer dissociation and structural changes in general. To investigate this effect, calculations of water density in the closed cavities (defined in Methods section) of a dimer and monomer were carried out for the chosen pressures. For every pressure, a set of calculations was carried out with varying radius of the boundary sphere from 6 to 20 Å for dimer and from 6 to 16 Å for monomer. In these calculations the number of water molecules in the closed cavity was determined as well as the number of water

molecules in the same closed cavity projected to a region of bulk water. The situation is depicted in Figure 5. The ratio of these numbers represents the relative density of water in the closed cavity and is shown in Figure 6 as a function of the boundary sphere radius. For small radii the cavity-water

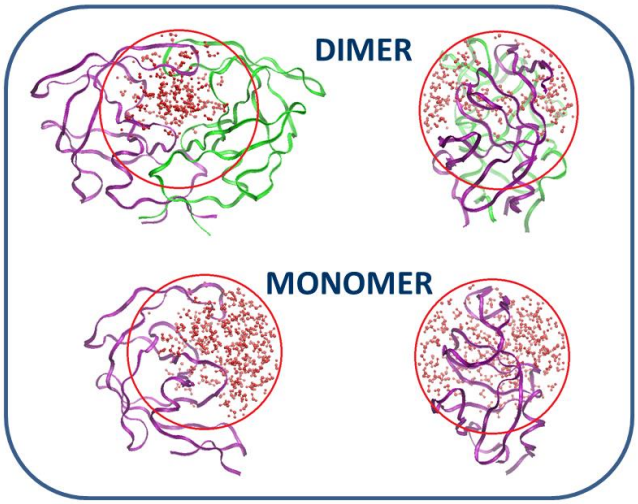

Figure 5. Water molecules (red) inside the closed cavity of a radius 14 Å in the molecules of HIV-1 PR dimer and monomer. Left images – front view, right images – side view.

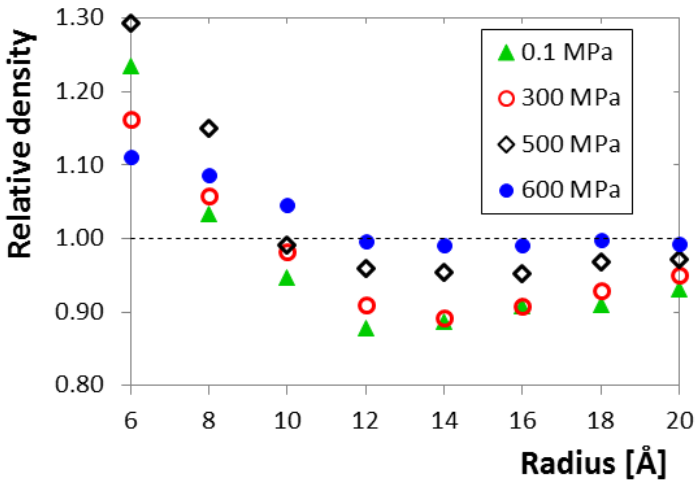

Figure 6. Relative density of water as a function of the boundary-sphere radius for selected pressures. Standard deviations of the mean of the individual points do not exceed 1.2% for the biggest sphere and 4.5% for the smallest sphere.

density is higher than that of free water but with growing radius it decreases quickly and the ratio gets reversed. At a certain radius, roughly corresponding with the real dimensions of the cavity, the density reaches its minimum value and then slowly grows to the bulk-water value as a consequence of decreasing influence of the protein inside the relatively big sphere. The initial decrease can be attributed to the electrostriction effect that concentrates water molecules around the charged aspartate residues. Indeed, the water density in the close proximity of the active-site aspartate residues exceeds significantly the bulk-water density and does not show any clear trend with changing pressure. Table 2 shows the relative density of water in a small closed cavity of a boundary-sphere radius of 6 Å. On the contrary, repulsion of water from the hydrophobic amino-acid residues constituting the inner surface of the cavity lowers the density of water at its walls. The minimum value was, therefore, taken as the average water density inside the cavity. Figure 7 shows that for the pressure up to about 200 MPa the density of water remains approximately constant at about 87% of the bulk water density. When the pressure is continuously increased up to 600 MPa, the density grows rapidly towards the bulk-water value.

Table 2. Relative density of water in the closed cavity of dimer with boundary-sphere radius of 6 Å.

pressure [MPa]	relative density
0.1	1.23
100	1.17
200	1.13
300	1.16
400	1.20
500	1.29
600	1.11

An analogous calculation for HIV-1 PR monomer revealed a similar trend, but the curve is shifted to much lower values of pressure. At atmospheric pressure the density is at about 96% of the bulk-water value and grows rapidly with increasing pressure approaching the bulk-water density closely between 100 and 200 MPa (Figure 7).

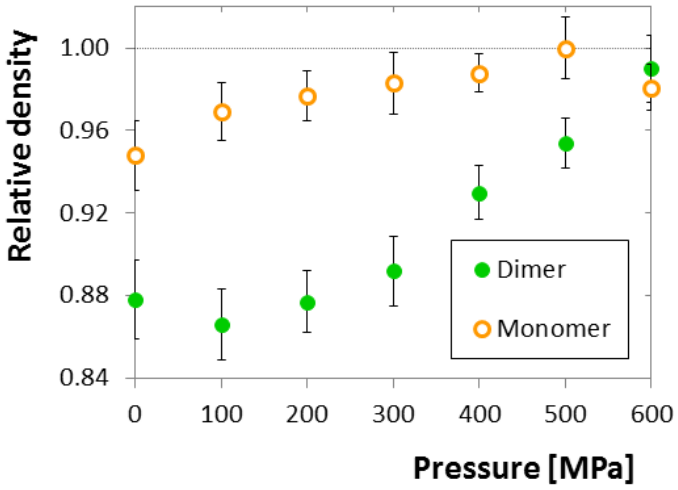

Figure 7. Relative density of water in the closed cavity of dimer and monomer. Relative density is calculated as a ratio of the number of water molecules in the respective closed cavity and the same closed cavity projected to the bulk-water region. Standard deviations of the data are indicated by the error bars.

These results indicate that the strongly curved hydrophobic inner surface of the active-site cavity repels some water from the interior. This effect remains almost constant up to the pressure of 200 MPa showing that the cohesive forces among the water molecules are strong enough to oppose the pressure tending to push them into the hydrophobic regions of the cavity. However, when the pressure is increased even higher, the cohesion of water is no more able to stand the external force and water begins to fill the cavity continuously. At the highest pressure considered in the simulation, 600 MPa, the external forces are so strong that there is no difference between the water inside and outside the cavity. For monomer the dependence is much weaker and the steepest increase of the density occurs at much lower pressure. The curvature of the concave shape

remaining after splitting the active-site cavity to two parts is thus insufficient to facilitate equally strong effect as the dimer cavity, but is still able of a weaker repulsion of water molecules which is almost negligible above 200 MPa.

An interesting comparison of monomer's and dimer's interaction with water follows from relating the water-accessible surface area to the number of water molecules located up to 3 Å from the surface. For lower pressures the dimer value is slightly higher while for higher pressures the values for dimer and monomer are approaching one another (data not shown). It can be explained by the stronger repulsion of water from the hydrophobic cavity of a dimer than from the monomer surface, which is in agreement with the calculation of average water density at both the molecular forms.

Additional calculations were carried out in order to evaluate the ratio of the numbers of water molecules located in the proximity of the hydrophilic and hydrophobic parts of the surface. Figure 8

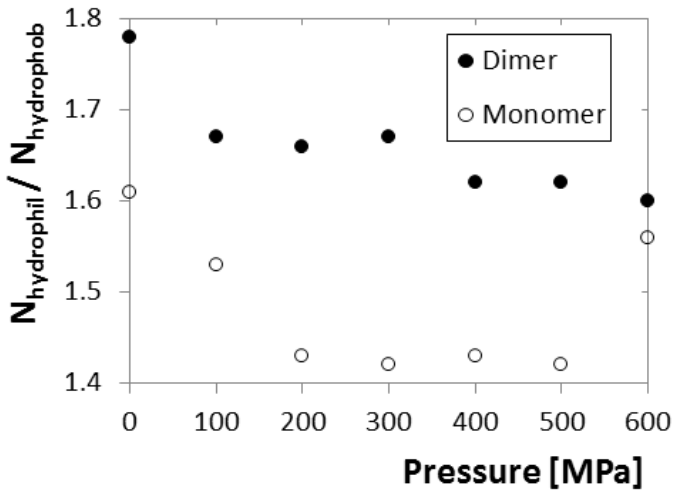

Figure 8. Ratio of water molecules at the hydrophilic and hydrophobic parts of the HIV-1 PR dimer and monomer surfaces. Standard deviations of the mean of the individual points do not exceed 0.3%.

presents this quantity for both dimer and monomer. Although it decreases almost equally for

monomer and dimer up to 100 MPa, probably due to hydration of analogous surface regions, a principle difference occurs at this pressure. For monomer the rapid decrease continues reaching its minimum value at 200 MPa and then remains constant, for dimer the decrease is rather slow with the steepest descent between 300 and 400 MPa. The observed behavior corresponds well with the calculated pressure profiles of monomer- and dimer-associated water densities. Hence, it can be assumed that the hydrophobic cavity has the most significant influence on the redistribution of water in the surroundings of the dimer and is mostly responsible for the total-volume change of the dimer to monomers dissociation.

2.3. Volume change of dimer dissociation

A principal point regarding the relation between computer simulations and experimental approach of dimer-monomer equilibrium under high pressure is the sign and magnitude of the volume change ΔV accompanying the dissociation of dimer to monomers, because it is a measure of the pressure dependence of the equilibrium constant of this process. Considering the rigidity of both the dimer and monomer structures, this volume change is presumably facilitated especially by interaction of the protein molecule with water. As discussed previously, the water density inside the active-site cavity can strongly depend on the pressure forcing the molecules inside against the repelling hydrophobic force.

Direct calculation of the volume change is rather troublesome as it is too small in comparison with the volumes of both the solvated dimer and monomers and even the volume fluctuations of the system. Nevertheless, an attempt was made to calculate it as a difference of PMVs of the dimer and two monomers. The resulting partial molecular volumes of both the systems are shown in Figure S4. For both dimer and monomer it decreases along with the growing pressure in a similar way in the order of hundreds to thousands $Å^3$. This decrease is likely caused by the reorganization of the

solvation sphere of the protein molecules, especially at the hydrophobic parts of their surfaces. Figure S3 shows the time development of the volume of the water box of the HIV-1 PR dimer at various pressures. Obviously, the obtained partial molecular volumes of both the systems (dimer and two monomers) are significantly higher than the volume fluctuations of the water box which allows us to calculate the partial molecular volumes with sufficient accuracy. However, the resulting molar volume changes ΔV_{PMV} are biased by rather high standard deviations which makes the trends of this quantity unclear (Figure S5). Nevertheless, their values are in the order of tens ml/mol for all the pressures under study, which is in agreement with the analogous experimental data for different proteins related to their molecular weight[32, 33].

To circumvent this problem of high volume fluctuations, a different approach was used that is focused on the local surroundings of the active-site cavity. The calculation is based on the assumption of different numbers of water molecules in the real closed cavity and in the closed cavity projected to the free water region. The latter state simulates a hypothetical ideal solution in which the interactions of a water molecule with its surroundings are equal at any point of the system. In such state water surrounds the protein uniformly, therefore the total volume of a system composed of an HIV-1 PR molecule and a certain number of water molecules has equal volume in both dimeric and monomeric state provided that the monomer shape is unchanged in both the states. When some molecules are repelled from the protein's closed cavity by the real intermolecular interactions, each of them increases the volume of the surrounding water by the volume it occupies in the bulk water. In order to eliminate the influence of the outer surface of the molecules that is assumed to be equal for dimer and free monomers, the closed cavities of both monomer and dimer were composed of a boundary sphere of equal radius of 14 Å which corresponds with the minimum of the relative water density in the dimer cavity for most of the pressures. Table 3 summarizes the input data of the calculation of ΔV and its resulting pressure dependence is shown in Figure 9A. The volume change is positive (i.e. the dissociation is accompanied with volume increase) in the

lower part of the pressure interval but decreases rapidly with growing pressure and turns to negative values at about 80 MPa. It reaches a minimum at 300 MPa and then grows back to zero or even small positive values at the highest pressure considered.

Table 3. Input parameters of the calculation of the volume change of HIV-1 PR dimer dissociation as functions of pressure. The data were calculated for the boundary sphere of 14Å radius where the water density in dimer closed cavity reached its minimum.

pressure [MPa]	$V_{m,H_2O,bulk}$ [a] [ml/mol]	$\Delta N_{H_2O,dim}$ [b]	$\Delta N_{H_2O,mon}$ [c]
0.1	18.08 (18.14)	14.7	11.0
100	17.21 (17.46)	18.7	7.3
200	16.67 (16.92)	15.7	5.3
300	16.19 (16.49)	14.7	4.0
400	15.93 (16.13)	9.7	2.7
500	15.64 (15.81)	6.0	0.0
600	15.42 (15.52)	1.3	4.3

[a] Molar volume of free water. The calculated values agree well with the experimental data[34] (in parentheses) and thus confirm the reliability of the used model of water.

[b] The number of water molecules inside the closed cavity of the dimer projected to the bulk-water region minus the number of water molecules in the real closed cavity of the dimer.

[c] The number of water molecules inside the closed cavity of the monomer projected to the bulk-water region minus the number of water molecules in the real closed cavity of the monomer.

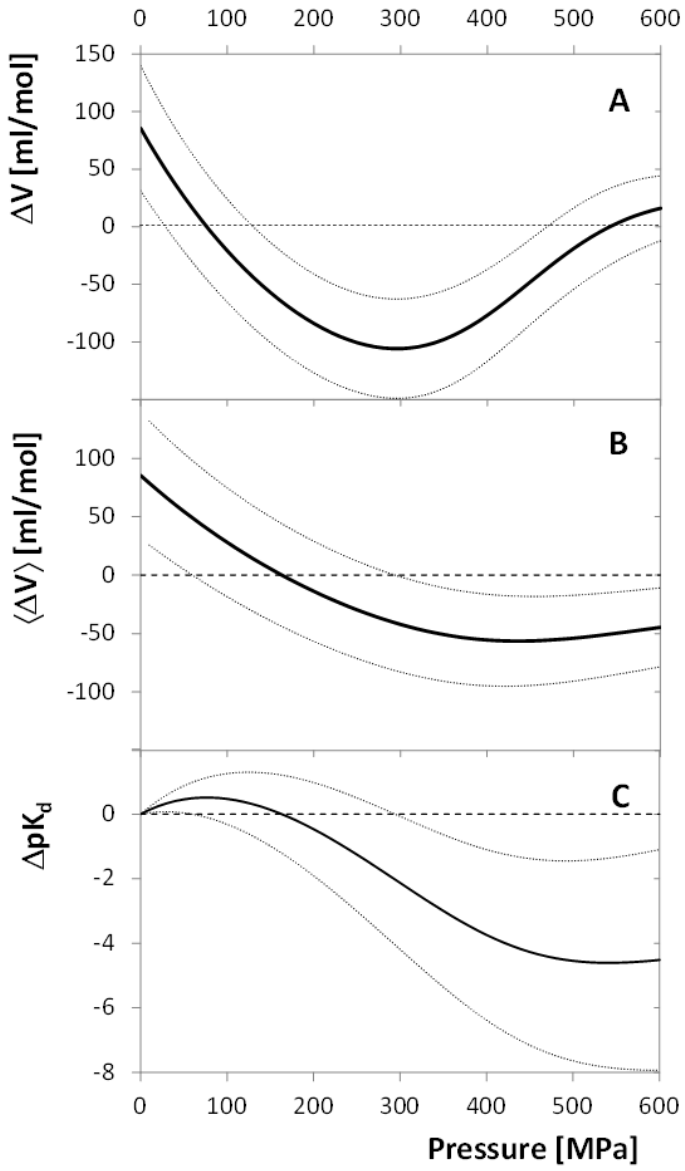

Figure 9. Volume change of the dimer dissociation and the shift of equilibrium constant K_d as functions of pressure. Standard deviations are indicated by the dotted lines. A. Volume change of the dimer dissociation. B. Average volume change in the interval from atmospheric to the given pressure. C. The shift of the equilibrium constant expressed in logarithmic scale as ΔpK_d.

The described behavior of ΔV can be explained as follows. The curved inner surface of the dimer cavity has a higher ability to repel water than only its half contained by the monomer. The monomer curvature is obviously insufficient to counteract pressure above 200 MPa, but still it can repel water

at lower pressures. Dimer cavity, on the other hand, is almost equally hydrophobic up to 200 MPa above which the water-repelling ability decreases, too. The minimum of ΔV occurs in a point where the monomer surface is almost completely filled with water, while the cavity of dimer is still highly hydrophobic. At low pressures the number of molecules repelled by dimer is approximately equal or even slightly lower than the number of molecules repelled by two monomers. This might be a consequence of a strong attraction of water by the two active-site aspartate residues bearing two closely located negative charges. Therefore, ΔV can reach even positive values. On the contrary, the positive ΔV at the upper end of the pressure range might be rather a consequence of a partial structural distortion of monomer that occurs at 600 MPa.

A common practice in the high-pressure experimental studies is to consider the volume change to be constant over the whole pressure range, often due to the limited sensitivity of the experimental devices. In order to enable the comparison of the current simulations with experiment, mean values of ΔV, defined as

$$\langle \Delta V \rangle = \frac{\int_{p_{atm}}^{p} \Delta V(p')dp'}{p - p_{atm}}, \qquad (1)$$

were calculated. Figure 9B shows that the dependence of $\langle \Delta V \rangle$ on pressure is smoother than that of ΔV itself. The transition from positive to negative values occurs at 160 MPa. Above this pressure $\langle \Delta V \rangle$ stays in the order of tens ml/mol, mostly between 20 and 60 ml/mol. This value corresponds well with our so far unpublished experimental data indicating ΔV of the same order of magnitude.

A principal experimental quantity that depends on ΔV is the equilibrium constant K_d. If ΔV is positive, high pressure shifts K_d to lower values, i.e. stabilizes the dimeric state, while with negative ΔV the situation is opposite. The shift of the equilibrium constant expressed as $\Delta pK_d(p)$ was evaluated according to Eq. (14) and is plotted in Figure 9C. At lower pressures up to 160 MPa

$\Delta pK_d(p)$ is slightly positive, the increased pressure therefore stabilizes the dimer in this range. However, at higher pressures this quantity is negative with significantly higher absolute values indicating a strong destabilization of dimer by high pressure. High pressure can therefore help the experimental techniques to observe monomeric HIV-1 PR in higher concentrations and thus with better signal to noise ratio.

Standard errors shown in Figure 9 indicate some inaccuracy in determination of ΔV and ΔpK_d which is a consequence of random fluctuations in the number of water molecules in the individual simulation frames. However, in spite of this the trends remain clear and the resulting curves provide a reasonable estimate of the high-pressure behavior of HIV-1 PR.

2.4. Protein-ion interactions

An interesting phenomenon is the stabilization of the active site by interaction of the two aspartate residues with a sodium cation. It was shown previously[35] and was also confirmed by our calculations that the interaction is highly favourable at atmospheric pressure as the interaction partially compensates the strong repulsion of the negatively charged aspartate residues. Thus, even if the simulation starts from a state without a sodium cation bound in the active site, it is often trapped by the aspartates and the system reaches equilibrium in this state. On the contrary, for the high pressure of 500 or 600 MPa the tendency of binding the cation is much weaker – in some runs of the simulation it is not trapped at all, while in others the cation sits to one of the residues, stays there for some time and then leaves. Only rarely the firm complex of the sodium cation with both Asp residues is formed. Moreover, in some cases escape of the cation from the bound state was observed. It indicates that the equilibrium between the states of free active site and the active site

bound with the cation is not strongly shifted to one or the other side at high pressure. This can be explained in a following way. The free Asp residues of the active site strongly attract the polar water molecules in order to compensate the mutual repulsion. This leads to the formation of a dense solvation sphere around these two residues, as can be seen in Table 2. When the ion is trapped by the two residues, it strongly contributes to the charge compensation and some water molecules leave the solvation sphere. At low pressure both the enthalpic contribution and the entropy increase of the released water molecules strongly favours the ion trapping by the aspartates. However, at high pressure this stabilizing effect can be overwhelmed by the influence of the volume growth when the water molecules pass from the highly organized solvation sphere to the bulk water of lower density. Therefore, formation of the Asp25-Asp25'-Na^+ complex can be less favourable at high pressures. At the intermediate pressures no apparent trend of the tendency of the active site to bind the cation was observed within the time scale of the simulation, but this phenomenon deserves further investigation.

3. METHODS

3.1. Model construction and MD equilibrium simulations

The structural stability of a HIV-1 PR dimer and monomer were studied by all-atom molecular dynamics (MD) simulations, where the solvent molecules were represented by an explicit solvent model. Simulations were performed in the pressure series of 0.1, 100, 200, 300, 400, 500, and 600 MPa at constant temperature of 310 K. The model was based on the X-ray crystal structure obtained from RCSB protein data bank (PDB ID: 1OHR)[36]. The inhibitor and the crystallographic water molecules were deleted from the source PDB file and hydrogens were added. Topology file has been constructed by NAMD automatic PSF builder. The dimer model was solvated with TIP3P[37] water and neutralized by adding 4 Cl^- ions. NaCl concentration was set to 0.20 mol/L. Initial

simulations of the dimer aimed at demonstration of the equilibrium properties of the system were performed with a water box of the dimensions 74.2 x 57.2 x 57.5 $Å^3$ ("smaller water box") for 54 ns and the pressures of 0.1 and 500 MPa. In case of the following simulations used for the calculation of the studied molecular properties the water box of the dimensions of 115.0 x 97.8 x 98.1 $Å^3$ ("bigger water box") contained 3 128 atoms of the protein, 35 664 water molecules, 134 Na^+ ions and 138 Cl^-, i.e. 110392 atoms in total. The monomer model was solvated by TIP3P water molecules and NaCl concentration was set to 0.20 mol/L, i.e. equally as in the dimer case. The water box of the dimensions of 96.9 x 84.3 x 97.8 $Å^3$ contained 1 564 atoms of the protein, 26 169 water molecules, 99 Na^+ ions and 101 Cl^- ions, i.e. 80271 atoms in total.

In accord with previous high-pressure molecular-dynamics studies[24-26], all simulations were performed using NAMD Version 2.9 program package[38] with the CHARMM22/CMAP topology and force-field parameters[39,40]. Timestep of 1 fs, 10 Å cutoff of the non-bonding interactions and a switching function starting at a distance of 8 Å were used. Full electrostatic calculations were performed using the Particle Mesh Ewald method (PME) implemented in the NAMD package. Native contacts between pairs of atoms (i,j) with $|i-j| < 4$ were discarded from the native contact list (1-4 scaling). Energy of the system was minimized for 180 fs prior to each MD simulation which was subsequently carried out at the constant temperature of 310 K and the selected pressure using periodic boundary conditions in the isobaric-isothermal (NPT) ensemble. The temperature was controlled using Langevin dynamics and the pressure was controlled using the Langevin piston Nosé-Hoover method. The piston oscilation period was 100 fs, the barostat damping decay was 50 fs. The length of the simulation runs was between 18 and 40 ns for different systems.

Interatomic distances and other geometric properties were evaluated by the VMD 1.9.1[41] program as average values over all frames of the selected part of the simulation where the system stayed in the closed conformation for a sufficient time period.

3.2. Water density and dimer-dissociation volume change calculation

In order to calculate the ratio of water density inside the active-site cavity and the density of bulk water located out of the reach of the protein-water interactions (hereafter called "relative density"), a boundary sphere of a selected radius centered in the geometric center of the α-carbons of Asp 25, Ala 28 and Pro 79 of both chains was constructed in order to define the active-site cavity borders. Analogously, a boundary sphere centered in the geometric center of the α-carbons of Asp 25, Ala 28, Ile 50 and Pro 79 was constructed around the concave shaped half-cavity of a monomer. The boundary of the region of interest (hereafter called "closed cavity") is then formed by either the van der Waals surface of the protein atoms or the boundary-sphere surface depending on what is closer to the sphere centre in a given radial direction. The atoms of the water molecules inside the closed cavity are counted. In case that a molecule sticks out of the cavity through the boundary sphere, only the inner atoms are taken into account. In a simultaneous calculation the closed cavity was projected geometrically to an arbitrarily chosen location in which the bulk water was unperturbed by the interactions with the protein. The atoms of water-molecules located inside the projected closed cavity were counted. In this case, molecules protruding through the boundary-sphere surface were treated as previously, but those protruding through the van der Waals surface of the protein atoms were excluded from the count completely. The number of water molecules in the projected and real closed cavities N_{proj} and N_{real}, respectively, were calculated as 1/3 of the water atoms present in the respective regions and their ratio, N_{real}/N_{proj}, which is equal to the relative density of water in the closed cavity, was used as a measure of the hydrophobicity of the cavity. Furthermore, the difference

$$\Delta N_{H_2O,dim} = N_{proj,dim} - N_{real,dim} \qquad (2)$$

was defined which is equal to the number of water molecules repelled by the hydrophobic surface

of the cavity of dimer with respect to a hypothetic reference state of no hydrophobic interaction, i.e. of equal density of water in every point of the system except the space occupied by the protein. Analogous quantities were defined for the monomer:

$$\Delta N_{H_2O,mon} = N_{proj,mon} - N_{real,mon}. \quad (3)$$

Finally, the number of water molecules repelled by a dimer was subtracted from the number of molecules repelled by two monomers giving the change in the number of repelled molecules during the dimer-dissociation process:

$$\Delta N_{H_2O,dissoc} = 2\Delta N_{H_2O,mon} - \Delta N_{H_2O,dim} \quad (4)$$

These quantities were evaluated by home-made program and were averaged over 10 frames selected from the well equilibrated parts of the simulation.

Molar volume $V_{m,H_2O,bulk}$ of unperturbed bulk water at the respective pressure was calculated as an Avogadro-number multiplied ratio of the volume of an arbitrarily chosen sphere positioned in the unperturbed bulk-water area and the number of water molecules located inside it.

In order to evaluate ΔV as a function of pressure in the whole range of 0.1 to 600 MPa the functions $\Delta N_{H_2O,dim}(p)$ and $\Delta N_{H_2O,mon}(p)$ were fitted by suitable smooth functions

$$\Delta N_{H_2O,dim}(p) = Q\frac{e^{-a(p-b)}}{1+e^{-a(p-b)}} \quad (5)$$

$$\Delta N_{H_2O,mon}(p) = Re^{-cp}, \quad (6)$$

where the parameters a, b, c, Q, R were obtained by means of non-linear regression. Accordingly,

$$\Delta N_{H_2O,dissoc}(p) = 2\Delta N_{H_2O,mon}(p) - \Delta N_{H_2O,dim}(p). \quad (7)$$

In addition, the molar volume of bulk water was fitted by a cubic polynomial

$$V_{m,H_2O,bulk}(p) = A + Bp + Cp^2 + Dp^3. \quad (8)$$

Non-linear regressions were performed in Wolfram Mathematica 9 program.

The resulting volume change of dimer dissociation $\Delta V(p)$ was calculated as

$$\Delta V(p) = \Delta N_{H_2O,dissoc}(p) V_{m,H_2O,bulk}(p). \quad (9)$$

Given the volume change, pressure dependence of the equilibrium constant of dimer dissociation

$$K_d = \frac{M^2}{D} \quad (10)$$

can be determined. As

$$K_d(p) = \exp\left(-\frac{\Delta G_r^0(p)}{RT}\right), \quad (11)$$

where $\Delta G_r^0(p)$ is the standard reaction change of the Gibbs energy at pressure p, and

$$\Delta G_r^0(p) = \Delta G_r^0(p_{atm}) + \int_{p_{atm}}^{p} \Delta V(p')dp' = \Delta G_r^0(p_{atm}) + \Delta G_{r,HP}^0(p), \quad (12)$$

the pressure dependence of K_d is

$$K_d(p) = \exp\left(-\frac{\Delta G_r^0(p_{atm}) + \Delta G_{r,HP}^0(p)}{RT}\right) = K_{d,atm} \exp\left(-\frac{\Delta G_{r,HP}^0(p)}{RT}\right). \quad (13)$$

Here $\Delta G_{r,HP}^0(p) = \int_{p_{atm}}^{p} \Delta V(p')dp'$. It is convenient to present the equilibrium-constant shift in the logarithmic scale, i.e.

$$pK_d(p) = pK_{d,atm} + \frac{\Delta G_{r,HP}^0(p)}{2.303RT} = pK_{d,atm} + \frac{\int_{p_{atm}}^{p} \Delta V(p')dp'}{2.303RT}, \quad (14)$$

where the pK quantities are conventionally defined as $-\log_{10} K$. The difference of pK_d for atmospheric pressure and given pressure p denoted $\Delta pK_d(p)$ is thus

$$\Delta pK_d(p) = \frac{\int_{p_{atm}}^{p} \Delta V(p')dp'}{2.303RT}. \quad (15)$$

3.3. Calculation of partial molar volumes

Total volumes of water boxes of dimer, monomer and free water were calculated averaging the

value over 5000 frames for dimer and monomer and 1000 frames for water. The water box of free water contained equal number of water molecules and ions as the water box of dimer except the ions compensating the protein charge. Average volume of one water molecule was evaluated. Partial molar volumes of dimer and monomer were calculated as a difference of the total volume of the water box of the respective system and the volume of the number of free-water molecules equal to the number of water molecules in this water box. Volume change of dimer dissociation ΔV_{PMV} (the index "PMV" was used to distinguish this quantity from ΔV defined in section 3.2.) was evaluated as

$$\Delta V_{PMV} = 2\,PMV(monomer) - PMV(dimer). \qquad (16)$$

4. CONCLUSIONS

High-pressure responses of HIV-1 PR dimer and monomer were investigated by molecular dynamics methods. Within the simulation time scale the conformations of both the forms are stable up to 500 MPa with only minor changes of the outermost surface domains around Pro39. Partial structural distortion of monomer can be seen at 600 MPa. With growing pressure the water molecules approach the protein surface even at the hydrophobic regions. An interesting consequence of this phenomenon is observed at the active-site cavity. There, the density of water is approximately at 87% of the bulk-water value up to 200 MPa, after which it starts to grow up reaching the bulk-water density at about 600 MPa. A similar, but weaker effect can be seen also at the monomer molecule. The difference of both these effects gives rise to the volume change of dimer dissociation which is positive at low pressures but changes the sign at 80 MPa, reaches minimum at 300 MPa and then returns to zero between 500 and 600 MPa. The dimer is thus slightly stabilized at the lower part of the pressure range but strongly destabilized at higher pressures. The equilibrium constant of dimer dissociation is thus shifted to higher values by high pressure, which can enable experimental studies of HIV-1 PR dimerization at higher concentrations and thus with

improved accuracy of the detection methods. Generally, high-pressure methods can play a role of helpful tools of investigation of oligomerization equilibria of proteins possessing hydrophobic cavities at the interfaces of their subunits.

ACKNOWLEDGMENTS

NAMD was developed by the Theoretical Biophysics Group in the Beckman Institute for Advanced Science and Technology at the University of Illinois at Urbana-Champaign.
(http://www.ks.uiuc.edu/Research/namd/)
VMD has been developed by the Theoretical and Computational Biophysics Group at the Beckman Institute for Advanced Science and Technology of the University of Illinois at Urbana-Champaign.
This work is supported by the National Institutes of Health under grant number P41-RR005969.

REFERENCES

1 M. Kožíšek, J. Bray, P. Řezáčová, K. Šašková, J. Brynda, J. Pokorná, F. Mammano, L. Rulíšek, J. Konvalinka, *J. Mol. Biol.* 2007, **374**, 1005–1016.

2 M. Kožíšek, K. G. Šašková, P. Řezáčová, J. Brynda, N. M. van Maarseveen, D. De Jong, C. A. Boucher, R. M. Kagan, M. Nijhuis, J. Konvalinka, *J. Virol.* 2008, **82**, 5869–5878.

3 A. Wlodawer, J. Vondrasek, *Annu. Rev. Bioph. Biom.* 1998, **27**, 249–284.

4 M. J. Todd, N. Semo, E. Freire, *J. Mol. Biol.* 1998, **283**, 475–488.

5 V. Veverka, H. Bauerova, A. Zabransky, J. Lang, T. Ruml, I. Pichova, R. Hrabal, *J. Mol. Biol.* 2003, **333**, 771–780.

6 R. Ishima, D. A. Torchia, J. M. Louis, *J. Biol. Chem.* 2007, **282**, 17190–17199.

7 J. M. Louis, R. Ishima, A. Aniana, J. M. Sayer, *Protein Sci*. 2009, **18**, 2442–2453.

8 Y. Levy, A. Caflisch, J. N. Onuchic, P. G. Wolynes, *J. Mol. Biol.* 2004, **340**, 67–79.

9 M. C. Yan, Y. Sha, J. Wang, X. Q. Xiong, J. H. Ren, M. S. Cheng, *Proteins* 2008, **70**, 731–738.

10 A. F. Noel, O. Bilsel, A. Kundu, Y. Wu, J. A. Zitzewitz, C. R. Matthews, *J. Mol. Biol.* 2009, **387**, 1002–1016.

11 M. Cavallari, C. Ghio, S. Monti, M. Ferrario, A. Maritan, P. Carloni, *J. Mol. Struc.–THEOCHEM* 2006, **769**, 111–121.

12 M. Bonomi, A. Barducci, F. L. Gervasio, M. Parrinello, *PLoS One* 2010, **5**, e13208.

13 H. J. Schramm, J. Boetzel, J. Buttner, E. Fritsche, W. Gohring, E. Jaeger, S. Konig, O. Thumfart, T. Wenger, N. E. Nagel, W. Schramm, *Antivir. Res.* 1996, **30**, 155–170.

14 T. F. Holzman, W. E. Kohlbrenner, D. Weigl, J. Rittenhouse, D. Kempf, J. Erickson, *J. Biol. Chem.* 1991, **266**, 19217–19220.

15 E. M. Towler, S. V. Gulnik, T. N. Bhat, D. Xie, E. Gustschina, T. R. Sumpter, N. Robertson, C. Jones, M. Sauter, N. Mueller-Lantzsch, C. Debouck, J. W. Erickson. *Biochemistry* 1998, **37**, 17137–17144.

16 C. A. Pargellis, M. N. Morelock, E. T. Graham, P. Kinkade, S. Pav, K. Lubbe, D. Lamarre, P. C. Anderson, *Biochemistry* 1994, **33**, 12527–12534.

17 P. L. Darke, S. P. Jordan, D. L. Hall, J. A. Zugay, J. A. Shafer, L. C. Kuo, *Biochemistry* 1994, **33**, 98–105.

18 M. Ingr, T. Uhlikova, K. Strisovsky, E. Majerova, J. Konvalinka, *Protein Sci*. 2003, **12**, 2173–2182.

19 E. Girard, S. Marchal, J. Perez, S. Finet, R. Kahn., R. Fourme, G. Marassio, A. C. Dhaussy, T. Prange, M. Giffard, F. Dulin, F. Bonnete, R. Lange, J. H. Abraini, M. Mezouar, N. Collo-c'h, *Biophys. J.* 2010, **98**, 2365–2373.

20 S. Marchal, A. Marabotti, M. Staiano, A. Varriale, T. Domaschke, R. Lange, S. D'Auria, *PLoS One*, 2012, **7**, e50489.

21 S. Sarupria, T. Ghosh, A. E. García, S. Garde, *Proteins* 2010, **78**, 1641-1651.

22 D. Paschek, A. E. García, *Phys. Rev. Lett*. 2004, **93**, 238105.

23 N. Smolin, R. Winter, *BBA-Proteins Proteom.* 2006, **1764**, 522-534.

24 T. Yamazaki, T. Imai, F. Hirata, A. Kovalenko, *J. Phys. Chem. B* 2007, **111**, 1206-1212.

25 A. Paliwal, D. Asthagiri, D. P. Bossev, M. E. Paulaitis, *Biophys. J.* 2004, **87**, 3479-3492.

26 J. A. Yancey, N. A. Vellore, G. Collier, S. J. Stuart, R. A. Latour, *Biointerphases* 2010, **5**, 85-95.

27 E. Paci, *Biochim. Biophys. Acta* 2002, **1595**, 185-200.

28 A. Lerbret, A. Hédoux, B. Annighöfer, M.-C. Bellissent-Funel, *Proteins* 2013, **81**, 326-340.

29 B. R. Meher, M.V. Satish Kumar, Kausik Sen, in ICIT 2008: Proceedings of the 11th international konference on information technology; Panda, B.S., Nayak, A., eds.; 2008, 118–122.

30 V. Hornak, A. Okur, R. C. Rizzo, C. Simmerling, *P. Natl. Acad. Sci. USA* 2006, **103**, 915–920.

31 A. L. Perryman, J.-H. Lin, A. McCammon, *Protein. Sci.* 2004, **13**, 1108–1123.

32 M. J. Kornblatt, R. Lange, C. Balny, *Eur. J. Biochem.* 2004, **271**, 3897-3904.

33 K. C. Ruan, G. Weber, *Biochemistry* 1988, **27**, 3295-3301.

34 C. W. Burnham, J. R. Holloway, N. F. Davis, *Am. J. Sci.* 1969, **267-A**, 70-95.

35 D. Kovalskyy, V. Dubyna, A. E. Mark, A. Kornelyuk, *Proteins* 2005, **58**, 450–458.

36 S. W.Kaldor, V. J.Kalish, J. F. Davies 2nd., B. V. Shetty, J. E. Fritz, K. Appelt, J. A. Burgess, K. M. Campanale, N. Y. Chirgadze, D. K. Clawson, et al., *J. Med. Chem.* 1997, **40**, 3979–3985.

37 W. L. Jorgensen, J. Chandrasekhar, J. D. Madura, R. W. Impey, M. L. Klein, *J. Chem. Phys.* 1983, **79**, 926-935.

38 J. C. Phillips, R. Braun, W. Wang, J. Gumbart, E. Tajkhorshid, E. Villa, C. Chipot, R. D. Skeel, L. Kale, K. Schulten, *J. Comput. Chem.* 2005, **26**, 1781–1802.

39 A. D. MacKerell, Jr.,D. Bashford, M. Bellott, R. L. Dunbrack, Jr., J. D. Evanseck, M. J. Field, S. Fischer, J. Gao, H. Guo, S. Ha, et. al., *J. Phys. Chem. B* 1998, **102**, 3586-3616.

40 A. D. MacKerell, M. Feig, C. L. Brooks, *J. Comput. Chem.* 2004, **25**, 1400-1415.

41 W. Humphrey, A. Dalke, K. Schulten, *J. Mol. Graphics* 1996, 14, 33–38.